JOURNAL OF VIROLOGY, Jan. 1990, p. 86–95
0022-538X/90/010086-10$02.00/0

Vol. 64, No. 1

Proviral DNA Integration and Transcriptional Patterns of Equine Infectious Anemia Virus during Persistent and Cytopathic Infections†

SIYAMAK RASTY,[1] BHARATI R. DHRUVA,[1] R. LOUIS SCHILTZ,[1] DING S. SHIH,[1] CHARLES J. ISSEL,[2] AND RONALD C. MONTELARO[1]*

Departments of Biochemistry[1] and Veterinary Science,[2] Louisiana State University, and the Louisiana Agricultural Experiment Station, Baton Rouge, Louisiana 70803-1806

Received 1 November 1988/Accepted 19 September 1989

The structure and integration patterns of equine infectious anemia virus (EIAV) proviral DNA and the patterns of viral transcription were examined in persistent and cytopathic infections of cultured cells. The results of Southern blot analyses indicated that, in persistently infected cells, about 30% of the EIAV provirus exists as randomly integrated DNA, while the remaining 70% is equally divided between unintegrated linear and closed circular forms. The cytopathic infection, in contrast, is characterized by levels of integrated provirus ranging from 65 to more than 90% of the total proviral DNA, depending on the extent of cytopathology exhibited by the virus strain employed. In both persistent and cytopathic infections, extensive Northern (RNA) blot analyses have revealed the presence of two major virus-specific transcripts, an 8.2-kilobase (kb) full-length genomic mRNA and a 3.5-kb single-spliced mRNA. A low-abundance 1.5-kb mRNA, presumably formed by a double-splicing event of the full-length RNA, was also detected in the cytopathic EIAV infection. The two major viral transcripts are present in approximately equal quantities in persistently infected cells, while the cytopathic infection reveals nearly a 30-fold higher level of viral transcripts in which the 3.5-kb species constitutes over 75% of the total viral mRNA. The relatively high proportion of proviral DNA integration and the simple pattern of viral transcription observed during EIAV infections appeared to be different from the generally observed patterns of predominantly unintegrated proviral DNA and multi-spliced viral mRNAs in cells infected with other lentiviruses such as visna virus or human immunodeficiency virus type 1. Moreover, the data suggested that the cytopathology of EIAV may be correlated in part with the degree of proviral DNA integration and levels of viral mRNA in infected cells, particularly that of the spliced 3.5-kb mRNA.

Persistent retrovirus infections constitute a major challenge in contemporary infectious disease research in both human and veterinary medicine. Although oncovirus and lentivirus infections have been of practical concern to veterinarians for decades, the recent discoveries of retroviruses associated with human leukemia and acquired immunodeficiency syndrome have generated a greater urgency for the development of procedures to control these types of viral infections. A prerequisite to this goal is the elucidation of the patterns of lentivirus proviral DNA replication and transcription and their correlation to viral persistence and pathogenesis.

Compared with oncoviruses, relatively little is known about the structure of lentivirus proviral DNA in infected cells and how different DNA forms might correlate with viral gene expression and pathogenesis. Although it is generally recognized that lentivirus-infected cells contain large quantities of extrachromosomal unintegrated viral DNA, no clear model has yet emerged as to the exact role of the integrated and unintegrated DNA forms in the establishment of disease during lentivirus infections. In the case of visna virus, it has been shown that infected sheep choroid plexus cell cultures contain both integrated and unintegrated viral DNA and that both forms are infectious in transfection experiments (5). However, other studies have revealed that in productive infections of sheep choroid plexus cell cultures with visna virus, cells lack any detectable integrated viral DNA (15). Furthermore, ongoing lentivirus studies continue to reveal increasingly more complex transcriptional patterns employed by these viruses. There is strong evidence that *trans* activation of gene expression, encoded by multispliced low-molecular-weight virus-specific transcripts, may be a property of lentiviruses in general on the basis of studies with visna virus and human immunodeficiency virus type 1 (HIV-1) (1, 2, 6, 21).

Among lentiviruses, equine infectious anemia virus (EIAV) offers a uniquely dynamic disease model for studying the flow of lentiviral genetic information and its relationship to viral persistence and pathogenesis. To date, however, very little is known about the structure of EIAV proviral DNA and its integration patterns in infected cells, and no studies have been reported on the transcriptional pattern of the virus. As a basis for future studies on the mechanism of EIAV gene expression during acute, chronic, and inapparent phases of equine infectious anemia in persistently infected horses, we have analyzed EIAV gene expression and its relationship to persistence and cytopathology in tissue culture. Specifically, we have determined the structure of EIAV proviral DNA and its transcriptional pattern in infected cells, using two distinct equine cell lines in which the virus establishes either a persistent or a cytopathic infection.

* Corresponding author.

† Approved for publication by the Director of the Louisiana Agricultural Experiment Station as manuscript number 88-12-2715.

MATERIALS AND METHODS

Cell cultures and virus strains. Primary cultures of fetal equine kidney (FEK) and fetal donkey dermal (FDD) cells were prepared and maintained as described previously (24). A prototype stock of EIAV, obtained by propagation of the Wyoming cell-adapted strain of EIAV (19) in FEK cells, was used to carry out infection of confluent monolayers of FEK or FDD cells at a multiplicity of infection of 1.0. In addition, an FDD-adapted stock of EIAV, prepared by propagation of prototype EIAV in FDD cells, was used to infect confluent monolayers of FDD cells at a multiplicity of infection of 1.0. Using repeated washes with phosphate-buffered saline containing 4 mM EDTA, infected FEK cells were harvested from roller bottles at 3 to 4 weeks postinfection, and infected FDD cells were recovered from flasks at the peak of the cytopathic effect (10 to 12 days after infection of FDD cells with FDD-adapted EIAV and 20 to 22 days after infection of FDD cells with prototype EIAV). For time course studies, various times after infection were used for recovery of infected FEK and FDD cells, as described below. Transformed canine fetal thymus cells (Cf2Th) and feline embryo fibroblasts (FEA) that were persistently infected with the Wyoming cell-adapted strain of EIAV were obtained from Larry Arthur (Program Resources, Inc., Fredrick Cancer Research Facility, Fredrick, Md.).

Isolation and purification of nucleic acids. Extrachromosomal DNA was prepared from the infected and uninfected cells by the Hirt procedure (16). After precipitation of chromosomal DNA, the supernatant and precipitate fractions were treated as follows. The supernatant fraction, containing the extrachromosomal DNA, was extracted once with phenol-chloroform, dialzyed against 10 mM Tris hydrochloride (pH 8.0)–10 mM EDTA (TE10), precipitated with ethanol, dissolved in TE10, and banded on a CsCl-ethidium bromide density gradient, using 0.9 g of CsCl per ml and 600 μg of ethidium bromide per ml. The chromosomal DNA precipitate was dissolved in TE10 and treated as the supernatant fraction, except that the CsCl concentration was 1.0 g/ml. After ultracentrifugation, the ethidium bromide and CsCl were removed by standard methods (20), and the chromosomal and extrachromosomal DNAs from the two fractions were precipitated with ethanol. Total cellular DNA and RNA were simultaneously isolated from the cells by a modification of the method of Chirgwin et al. (4; Bethesda Research Laboratories, Inc., BRL Focus 6:11, 1984). After ultracentrifugation, the viscous layer of DNA was recovered from the cellular homogenate, extracted with phenol-chloroform, and precipitated by ethanol. The DNA pellet was dissolved in 10 mM Tris hydrochloride (pH 8.0)–1 mM EDTA, treated with RNase A followed by proteinase K, extracted once with phenol-chloroform, and precipitated with ethanol (20). The pellet of RNA was suspended in 10 mM Tris hydrochloride (pH 7.5)–5 mM EDTA–1% sodium dodecyl sulfate (SDS), extracted twice with phenol-chloroform, and precipitated with ethanol. Poly(A)$^+$ RNA was purified by two cycles of oligo(dT)-cellulose chromatography of total cellular RNA (20) or by direct oligo(dT)-cellulose chromatography of cell lysates, using the Fast Track mRNA isolation kit from Invitrogen.

Construction and labeling of probes. Virus-specific DNA fragments were obtained by restriction digestion of an EIAV proviral DNA clone, lambda 12 (8, 28, 31). The fragments were isolated and purified by electrophoresis through low-melting-point agarose or polyacrylamide gels followed by chromatography through a NACS-52 resin (Bethesda Research Laboratories, Inc.) column and subcloned into various plasmid vectors according to standard recombinant DNA techniques (20). After amplification in *Escherichia coli*, the fragments were then gel purified and labeled with [α-^{32}P]dCTP to specific activities of greater than 5×10^8 cpm/μg. A 4.95-kilobase (kb) *Bam*HI fragment (see Fig. 1A), covering about 60% of the viral genome and the entire *gag-pol* coding region, was labeled via nick-translation (20) and used as the probe for Southern blot analysis of proviral DNA. For Northern (RNA) blot analysis of viral RNA, the following restriction fragments, schematically shown in Fig. 4, were labeled by random-primer labeling (10) and used as probes: probe A, 220-base-pair (bp) *Mlu*I-*Bam*HI; probe B, 395-bp *Pvu*II-*Kpn*I; probe C, 513-bp *Sma*I-*Sst*I; probe D, 105-bp *Pvu*II-*Ssp*I; probe E, 120-bp *Bam*HI-*Taq*I; probe F, 420-bp *Sph*I-*Xba*I; probe G, 325-bp *Ava*II.

Southern and Northern hybridization conditions. Five micrograms of each DNA sample was fractionated by electrophoresis through a 0.7% agarose gel in Tris-borate-EDTA buffer (20) at 40 V overnight. Transfer of DNA to nitrocellulose and prehybridization and hybridization conditions were as described earlier (25). For Northern hybridizations, 2.5 μg of poly(A)$^+$ RNA or 15.0 μg of total RNA from infected or uninfected cells was subjected to electrophoresis in 1.0 or 1.4% agarose-formaldehyde gels (20 by 20 cm) (20) in 50 mM MOPS (morpholinepropanesulfonic acid) (pH 7.0)–1 mM EDTA buffer. Electrophoresis was carried out at 100 V for 1 h without buffer circulation and at 30 V for 14 h with buffer circulation. To check for the integrity of RNA samples, the gels were stained by being soaked in a solution of 5.0 μg of ethidium bromide per ml of water for 5 min in the dark and destained for 3 to 8 h in water in the dark. For transfer of RNA, the staining step was omitted, and the gel was washed immediately after electrophoresis for 1 h in 10× SSC (1× is 0.15 M NaCl, 0.015 M sodium citrate) to remove the formaldehyde and transferred overnight to GeneScreen or GeneScreen Plus nylon membranes (New England Nuclear-DuPont) in 10× SSC. Prehybridization was carried out at 42°C for 2 to 4 h in a buffer containing 50% formamide–5× Denhardt (20)–6× SSC–1% SDS–250 μg of denatured salmon sperm DNA per ml–25 mM sodium phosphate (pH 6.5). Hybridization was carried out at 42°C for 18 to 24 h, using 10^6 cpm of ^{32}P-labeled probe per ml of hybridization solution, which contained the same composition as the prehybridization buffer except that 1× Denhardt was used. After hybridization, the membranes were washed for 30 min at room temperature in 2× SSC–0.2% SDS and for 30 min at 65°C in 0.2× SSC–0.2% SDS. The membranes were then analyzed by autoradiography at −70°C for 12 to 36 h.

Relative concentration and copy number of proviral DNA in infected cells. To determine the relative concentration and copy number of complete viral genomes in infected FEK and FDD cells, total cellular DNA was digested with *Mlu*I, an enzyme which cuts the proviral DNA only in the long terminal repeat (LTR) (8, 28; see Fig. 1A), resulting in a DNA fragment of about 8.0 kb in size. Five micrograms of *Mlu*I-digested total cellular DNA from infected FEK or FDD cells was subjected to Southern blot analysis, using the ^{32}P-labeled 4.95-kb *Bam*HI fragment as probe. To obtain a standard curve, known concentrations of a plasmid subclone which contains a 6.8-kb viral-specific *Hin*dIII fragment were used. The 6.8-kb insert of this plasmid contains about 5.6 kb of the viral genome attached to about 1.2 kb of cellular DNA sequences. The concentration of the *Hin*dIII-digested plasmid DNA was adjusted so that each lane on the gel repre-

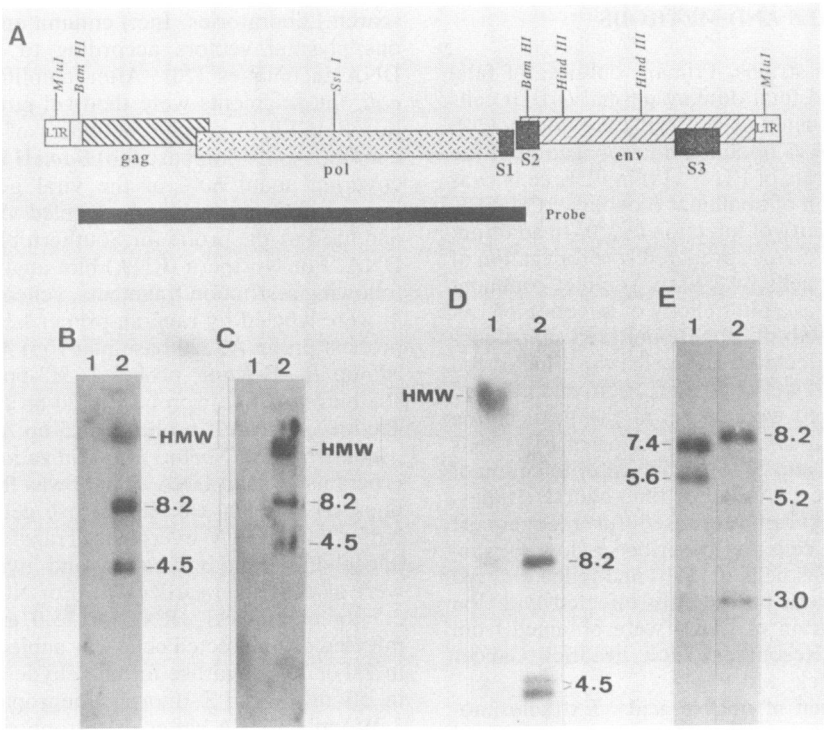

FIG. 1. Structural analysis of EIAV proviral DNA. (A) Diagram of the EIAV proviral genome based on its DNA sequence (28, 31), showing the location of the *Hin*dIII and *Sst*I restriction sites used for the structural analysis of unintegrated extrachromosomal proviral DNA. The unique *Mlu*I restriction sites, one in each LTR, are also shown. The solid black line represents the 4.95-kb *Bam*HI fragment used as the probe for Southern hybridization analyses shown in panels B, C, D, and E of this figure and panels A, B, and C of Fig. 3. (B and C) Southern blot of total undigested cellular DNA from uninfected FEK cells (panel B, lane 1), uninfected FDD cells (panel C, lane 1), prototype EIAV-infected FEK cells (panel B, lane 2), and prototype EIAV-infected FDD cells (panel C, lane 2). (D) Southern blot of the Hirt precipitate (lane 1) and Hirt supernatant (lane 2) DNA from prototype EIAV-infected FEK cells. (E) Southern blot of the Hirt supernatant DNA from prototype EIAV-infected FEK cells digested with *Hin*dIII (lane 1) or *Sst*I (lane 2). The number next to each hybridizing DNA species refers to its size in kilobases. HMW, High molecular weight.

sented 2.5×10^6, 5.0×10^6, 7.5×10^6, and 10.0×10^6 copy equivalents of viral genome.

EIAV LTR-CAT plasmid construction. A 478-bp *Bst*NI-*Pvu*II fragment, containing the EIAV 5′ LTR (8), was excised from the lambda 12 proviral DNA clone of EIAV and end repaired by treatment with T4 DNA polymerase. After the addition of *Hin*dIII linkers, the 5′-LTR fragment was subcloned into the unique *Hin*dIII site of pSV0CAT (13), and recombinants were identified by restriction enzyme mapping. DNA from the recombinant plasmid, pLTRCAT, was prepared by standard protocols (20) and subjected to two cycles of centrifugation through cesium chloride density gradients before use in transfection experiments.

Cells, transfections, and CAT assays. Uninfected or EIAV-infected FEA, Cf2Th, FEK, and FDD cells were seeded onto 60-mm-diameter petri plates at a density of 3×10^5 per plate and maintained in Eagle minimal essential medium supplemented with 10% fetal calf serum. Ten micrograms of pSV0CAT (negative control), pSV2CAT (positive control), or pLTRCAT plasmid DNA was transfected onto the cells as a calcium phosphate coprecipitate followed by a 15% glycerol shock, as described previously (12). FEA and Cf2Th cells were exposed to the plasmid DNA precipitate for 4 h, whereas the exposure of FEK and FDD cells to the precipitate was for 12 h. Transfected cells were incubated in a humidified 5% CO_2 incubator for 48 h, after which they were harvested and lysed by three cycles of freeze-thawing. Cell lysates were heat treated for 10 min before the assay for chloramphenicol acetyltransferase (CAT) activity to ensure the removal of endogenous cellular acylases. Then 10 μl of lysate from FEA, Cf2Th, and FDD cells and 50 μl of lysate from FEK cells was subjected to a kinetic CAT assay protocol, as described previously (23).

RESULTS

EIAV establishes a persistent, noncytopathic infection in FEK cells grown in tissue culture. In FDD cells, however, the virus causes a cytopathic infection characterized by rounding and detachment of infected cells. The time required for the appearance of cytopathologic changes is virus strain dependent. Prototype EIAV-infected FDD cells require 20 to 22 days to exhibit the complete cytopathic effect, while the same effect takes only 10 to 12 days to appear in FDD cells infected with the FDD-adapted strain of EIAV. To gain a better understanding of the patterns of EIAV gene expression during persistent and cytopathic infections, we analyzed the structure of EIAV proviral DNA and the transcriptional pattern of the virus during these infections.

Structural analysis of proviral DNA. Using a 4.95-kb *Bam*HI proviral DNA fragment as probe (Fig. 1A), Southern blot analysis of undigested total cellular DNA demonstrated the presence of three species of EIAV-specific DNA in FEK or FDD cells infected with prototype EIAV (Fig. 1B and C, respectively, lanes 2). One of these DNA species migrates as a high-molecular-weight form at a size range greater than 20

kb, while the other two have electrophoretic mobilities of about 8.2 and 4.5 kb. These DNA species were not detected in DNA isolated from uninfected FEK or FDD cells (Fig. 1B and C, respectively, lanes 1), indicating that the EIAV provirus is not endogenous to the equine genome. Using the procedure of Hirt (16), total cellular DNA from persistently infected FEK cells was fractionated into chromosomal and extrachromosomal DNA fractions and each fraction was analyzed by Southern blot hybridizations as above. As shown in Fig. 1D, both fractions show the presence of virus-specific sequences. The chromosomal DNA fraction reveals a high-molecular-weight viral DNA species migrating at a size range greater than 20 kb (Fig. 1D, lane 1), whereas the extrachromosomal fraction shows viral DNA migrating at about 8.2 and 4.5 kb (Fig. 1D, lane 2).

The structure of the extrachromosomal DNA was further analyzed by restriction enzyme digestions of the Hirt supernatant DNA from infected FEK cells followed by Southern hybridization analysis, using the 4.95-kb *Bam*HI fragment as probe. Digestion of the extrachromosomal DNA with *Hin*dIII, an enzyme which cuts the EIAV genome twice (Fig. 1A), produced two EIAV-specific hybridizing DNA fragments which migrate at 7.4 and 5.6 kb (Fig. 1E, lane 1). Moreover, digestion of the same DNA preparation with *Sst*I, an enzyme which cleaves the EIAV genome only once (Fig. 1A), resulted in three distinct viral DNA fragments of 8.2, 5.2, and 3.0 kb (Fig. 1E, lane 2). The restriction enzyme cleavage patterns are consistent with the extrachromosomal viral DNA species which migrates at 8.2 kb in Southern blots of undigested cellular DNA (Fig. 1B and C, lanes 2), being the linear form of the provirus which produces the 5.6-kb *Hin*dIII fragment and the 5.2- and 3.0-kb *Sst*I fragments. In contrast, the extrachromosomal DNA species migrating at 4.5 kb in the same blots appears to be a closed circular form of the provirus which produces the 7.4-kb *Hin*dIII fragment and the 8.2-kb *Sst*I fragment. The presence of a doublet at 4.5 kb (Fig. 1D, lane 2) may represent two distinct species of the closed circular provirus with one or two copies of the LTR (32), with the one-LTR circle being the predominant species.

Densitometric analysis of the three species of proviral DNA (integrated, linear, and circular) observed in EIAV infections revealed that during the persistent infection of FEK cells about 70% of the EIAV provirus is unintegrated, whereas nearly 30% of the proviral DNA is in the high-molecular-weight integrated form (Fig. 1B, lane 2). During the cytopathic infection of FDD cells, however, the predominant proviral DNA species is the integrated form, comprising nearly 65% of the total proviral DNA, while the remaining 35% is in the unintegrated form (Fig 1C, lane 2). The observation of such a relatively large proportion of the EIAV provirus in the integrated form during persistent infection of FEK cells and an even larger percentage during cytopathic infection of FDD cells is significantly different from the less than 1% integrated proviral DNA observed in productive infections with other lentiviruses such as visna virus (15).

As a second approach for quantitation of the three forms of EIAV provirus and a determination of the proviral copy number in infected cells, total cellular DNA from prototype EIAV-infected FEK or FDD cells was subjected to restriction enzyme digestion before Southern blot analysis. In so doing, we wished to eliminate the possibility of differential transfer efficiencies of the three different proviral DNA species from the agarose gel to the hybridization membrane. Total cellular DNA (chromosomal and extrachromosomal) isolated from FEK or FDD cells infected with prototype

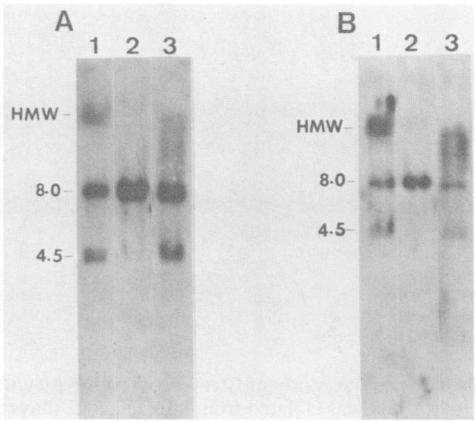

FIG. 2. Quantitation of the various EIAV proviral DNA forms. Southern blot analysis of total cellular DNA isolated from prototype EIAV-infected FEK (A) or FDD (B) cells. Lanes: 1, undigested DNA; 2, *Mlu*I-digested DNA; 3, *Eco*RI-digested DNA. The numbers next to the two lower hybridizing DNA bands are their sizes in kilobases. HMW, High molecular weight. The blots represent two separate experiments utilizing 5.0 μg of each DNA sample per lane and the full-length 8.2-kb EIAV proviral DNA as probe. The probe was later stripped from the blots, and the membranes were hybridized to a ^{32}P-labeled actin cDNA as an internal control. Densitometric analysis of the actin signal indicated that approximately equal quantities of DNA were present on the respective lanes of both membranes (data not shown).

EIAV was digested with *Mlu*I, an enzyme which cuts the EIAV provirus only in the LTR (Fig. 1A), and subjected to Southern blot analysis using a full-length proviral DNA probe. Following an *Mlu*I digestion, the integrated, closed circular, and full-length linear proviral DNA molecules all yielded an 8.0-kb linear DNA species (Fig. 2A and B, lane 2). Densitometric analysis of this 8.0-kb signal then yielded the sum of all proviral DNA molecules (integrated and unintegrated) in infected cells and revealed the total proviral copy number to be around nine copies per infected FEK or FDD cell (Table 1).

The relative percentage of the high-molecular-weight integrated provirus was then determined after digestion of total cellular DNA with *Eco*RI, an enzyme which does not cut the EIAV provirus and only digests the cellular junction sequences (28, 31). Southern blot analysis of the *Eco*RI-digested total cellular DNA revealed that the high-molecular-weight integrated proviral DNA, observed in undigested preparations of total DNA from infected cells (Fig. 2A and B, lanes 1), was converted by *Eco*RI into a heterogeneous population of hybridizing DNA fragments (Fig. 2A and B,

TABLE 1. Ratio of integrated to unintegrated EIAV proviral DNA in persistent versus cytopathic infections

EIAV-infected cell line	Proviral DNA copies in 5.0 μg of total cellular DNA[a]	% of cell population infected[b]	Proviral DNA copies per infected cell	% Integrated provirus[a]	Integrated/unintegrated proviral copies per infected cell
FEK	9	100	9	30	3/7
FDD	3	30	9	70	7/3

[a] Calculated from data in Fig. 2. Estimated values based on averages obtained from three separate experiments.

[b] Estimated values based on percentage of cells demonstrated to be infected with EIAV by immunofluorescence studies (C. J. Issel and R. C. Montelaro, unpublished data).

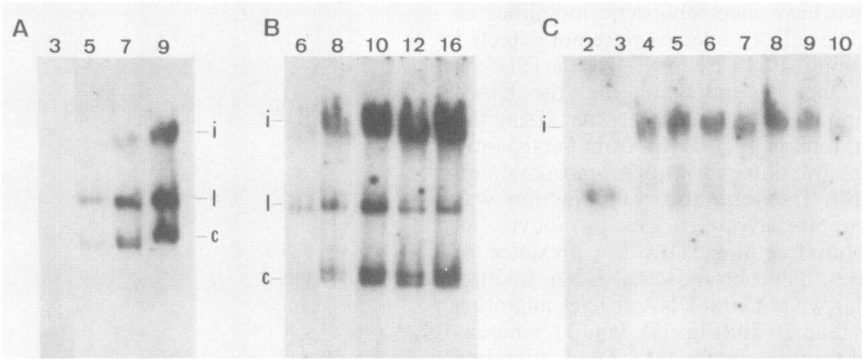

FIG. 3. Time course study of EIAV proviral DNA synthesis. The numbers above each lane in panels A, B, and C correspond to the times at which total DNA was isolated from infected cells (days postinfection). Abbreviations: i, integrated, l, linear, c, circular. (A) Southern blot of undigested total cellular DNA isolated from FEK cells persistently infected with prototype EIAV. (B) Southern blot of undigested total cellular DNA isolated from FDD cells infected with prototype EIAV. (C) Southern blot of undigested total cellular DNA isolated from FDD cells infected with FDD-adapted EIAV.

lanes 3), indicative of random integration sites of the EIAV provirus and a multitude of different cellular junction sequences. Densitometric analysis of this smear of hybridizing bands revealed that about 30% of the total proviral DNA molecules in infected FEK cells are integrated, while the integrated provirus constitutes around 65% of all viral DNA in infected FDD cells. Moreover, the percentage of the unintegrated linear proviral DNA was determined by densitometric analysis of the Southern blots of undigested total cellular DNA from infected FEK and FDD cells (Fig. 2A and B, lanes 1), in which the linear proviral DNA would transfer as efficiently as the other two forms of the provirus that were linearized by *Mlu*I (lane 2) or *Eco*RI (lane 3) in Fig. 2A and B. Such an analysis estimated the percentage of the unintegrated, full-length linear proviral DNA molecules to be about 40% of the total proviral DNA in infected FEK cells and around 20% of all proviral DNA in infected FDD cells. Finally, subtraction of the percentage of integrated and unintegrated linear proviral DNA from the total proviral DNA present in infected FEK or FDD cells indicated the percentage of closed circular unintegrated provirus to be about 30% in infected FEK cells and 15% in infected FDD cells. Thus, the ratios of integrated to unintegrated viral DNA obtained with digested preparations of total cellular DNA are in close agreement with those obtained by earlier analyses of undigested DNA.

Kinetics of proviral DNA synthesis. To ascertain whether the relatively high level of EIAV proviral DNA integration was a result of long-term infection, we performed a time course study to monitor the kinetics of proviral DNA synthesis after infection. Total cellular DNA was isolated from infected FEK cells on 3, 5, 7, and 9 days after infection, and 5.0 μg of undigested total DNA from each time point was analyzed by Southern blot hybridizations as before. The data in Fig. 3A indicate that the total proviral DNA in infected FEK cells increases in quantity as the infection proceeds and that the unintegrated form is the more abundant species from the onset of infection. However, it is also evident that the 30/70 ratio of integrated to unintegrated proviral DNA is established early during the persistent infection of FEK cells by EIAV. Parallel studies of the proviral DNA species during cytopathic infection of FDD cells by EIAV were also performed. A time course analysis of the formation of proviral DNA forms after the infection of FDD cells by prototype EIAV is presented in Fig. 3B. In this case, the integrated and unintegrated forms were detected simultaneously from the earliest time point at an approximate ratio of 70/30 integrated to unintegrated DNA. Taken together, these results indicate that the characteristic ratios of integrated to unintegrated EIAV DNA are established early in infection and are not a result of long-term culturing of infected cells.

The abundance of integrated proviral DNA during the cytopathic infection of FDD cells raised the possibility that the relative level of proviral DNA integration may correlate with EIAV cytopathology. To examine this hypothesis we studied the cytopathic infection of FDD cells with the FDD-adapted strain of EIAV, a strain which results in cytopathologic changes in half the time required by the prototype strain of the virus. During this rapid cytopathologic process, integrated proviral DNA was detected at an earlier stage of infection compared with prototype EIAV-infected FDD cells and its proportion eventually exceeded more than 90% of total viral DNA (Fig. 3C).

Thus, it appears that the cytopathologic changes observed after EIAV infection of FDD cells cannot be correlated with absolute levels of proviral DNA in infected cells, as there are approximately equal copies of the provirus during persistent or cytopathic infections of FEK or FDD cells, respectively (Table 1). However, the cytopathologic process may correlate with the ratio of integrated to unintegrated viral DNA in infected cells.

Northern blot analysis of viral RNA. In this set of experiments, we sought to define the patterns of viral transcription during cytopathic and persistent infections by EIAV. Viral transcripts were initially identified in FDD cells infected with the FDD-adapted strain of EIAV. Northern blots of poly(A)$^+$ RNA isolated from uninfected FDD cells or FDD cells infected with prototype EIAV at the peak of the cytopathic effect were hybridized to a 5′-specific probe representing sequences from the 5′ LTR of the EIAV genome. No virus-specific RNA species were detected in RNA from uninfected cells (Fig. 4, panel H), whereas three species of viral RNA were identified in RNA from infected FDD cells, an 8.2-kb genome-length RNA, a 3.5-kb RNA, and a low-abundance 1.5-kb RNA (Fig. 4, panels A1 and A2). Panel A1 is a Northern blot of a 1.4% agarose-formaldehyde gel, with the higher percentage gel resulting in a sharpened 1.5-kb hybridizing RNA band, while panel A2 is a blot of a 1.0% agarose-formaldehyde gel.

To further characterize the transcriptional pattern of EIAV, Northern blots of poly(A)$^+$ RNA from infected FDD

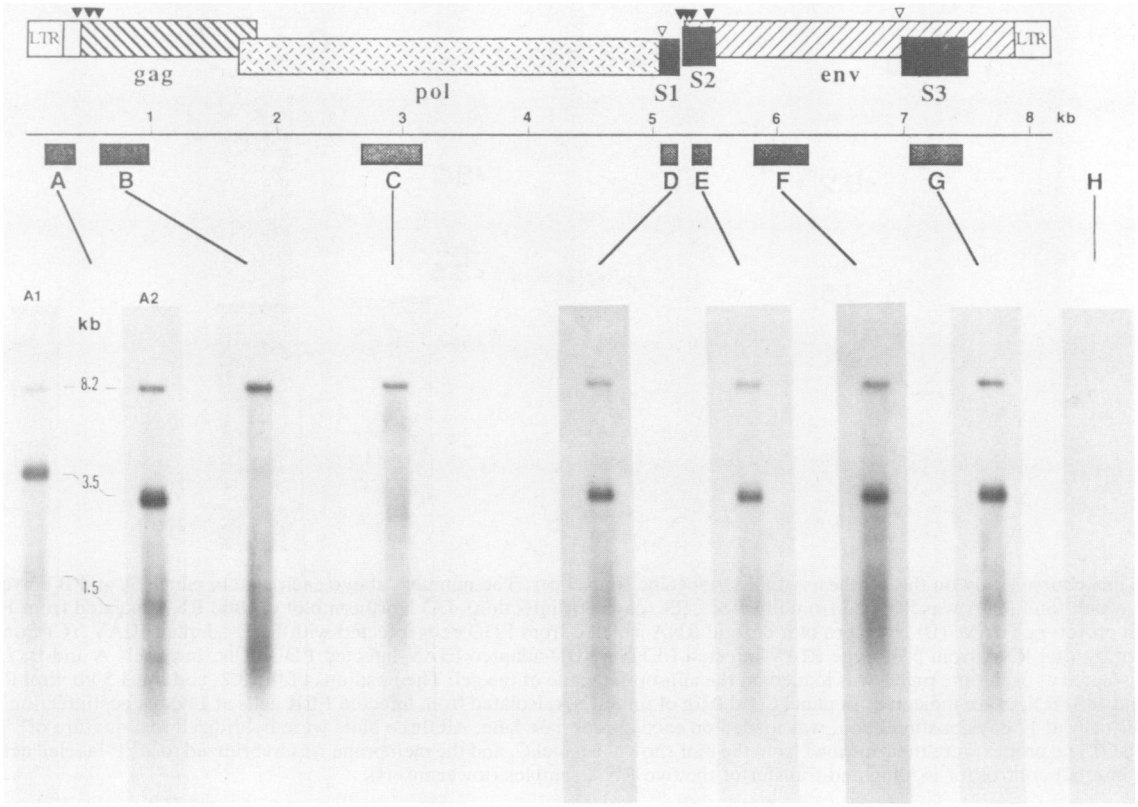

FIG. 4. Northern hybridization analysis of EIAV-specific transcripts in FDD cells infected with FDD-adapted EIAV. A diagram of the EIAV proviral DNA genome and the location of the six ORFs is represented at the top of the figure. Based on DNA sequence data (28, 31), closed triangles represent the location of consensus splice donor sites and open triangles represent the location of consensus splice acceptor sites. The stippled bars, labeled A through G, show the locations and sizes of the subgenomic probes relative to the EIAV genome. The bottom portion of the figure shows the results of hybridization of 2.5 μg of poly(A)$^+$ RNA from infected FDD cells, isolated at the peak of the cytopathic effect, to each of subgenomic probes A through G. (H) RNA from uninfected FDD cells. The positions of the 8.2-, 3.5-, and 1.5-kb viral mRNAs are indicated. Panel A1 represents a Northern blot of a 1.5% agarose-formaldehyde gel, while the remaining panels, including A2, are blots of a 1.0% gel. The molecular size marker used for this experiment was the 0.24- to 9.5-kb RNA ladder (Bethesda Research Laboratories, Inc.) which was run on a parallel lane, transferred, and hybridized to ^{32}P-labeled lambda DNA.

cells, run on a 1.0% agarose-formaldehyde gel, were hybridized to a panel of probes spanning the EIAV genome (probes B through G). As shown in Fig. 4, the *gag*- and the *pol*-specific probes (probes B and C) hybridized only to the full-length 8.2-kb viral RNA, indicating that this transcript represents both the *gag-pol* mRNA as well as the genomic RNA. The *env*-specific probe (probe F) hybridized to the full-length viral RNA in addition to the 3.5-kb RNA, suggesting that the 3.5-kb transcript may be the single-spliced mRNA encoding the EIAV *env* gene. Furthermore, each of the subgenomic probes representing sequences from the three short open reading frames (ORFs) *S1*, *S2*, and *S3* (9, 28) (probes D, E, and G) hybridized to all three virus-specific transcripts, suggesting that the 1.5-kb RNA is presumably a double-spliced message containing sequences from the 5′ end of the genome and each of ORFs *S1*, *S2*, and *S3*. However, in this cytopathic EIAV infection, the presence of only three detectable virus-specific RNAs and the abundance of the 3.5-kb transcript relative to the 8.2- or the 1.5-kb viral RNAs were significantly different from the complex transcriptional patterns of other lentiviruses such as HIV-1 or visna virus, in which a family of double-spliced viral transcripts are detected in levels equivalent to those of the full-length genomic and the single-spliced *env* mRNA species (2, 7, 22, 26, 33).

The differential steady-state levels of the viral RNAs detected late in this cytopathic EIAV infection could be attributed to a temporally regulated, differential splicing of the genome-length RNA, resulting in relatively different concentrations of the various viral RNA species late during the infection. To examine this possibility, a time course study was performed during which total cellular RNA isolated from FEK cells at 3, 5, 7, and 9 days after infection with prototype EIAV and from FDD cells at 2, 4, 6, 8, 10, and 12 days after infection with FDD-adapted EIAV was subjected to Northern blot analysis by using a mixture of probes A and G. As shown in Fig. 5A, no viral transcripts were detected in infected FEK cells until 9 days after infection and the earliest detectable RNA species, present at almost equal concentrations, were the full-length 8.2-kb and the spliced 3.5-kb transcripts. In infected FDD cells, however, viral transcripts were detectable as early as 2 days after infection and the increase in their concentrations reached a plateau at day 6 of infection (Fig. 5B). Furthermore, during this kinetic study of viral RNA synthesis in infected FDD cells, the concentration of the 3.5-kb RNA appeared to be about three times greater than that of the full-length transcript, even at the earliest time point, suggesting the presence of enhanced levels of 8.2-kb genome-length viral RNA splicing during this cytopathic EIAV infection. The low-

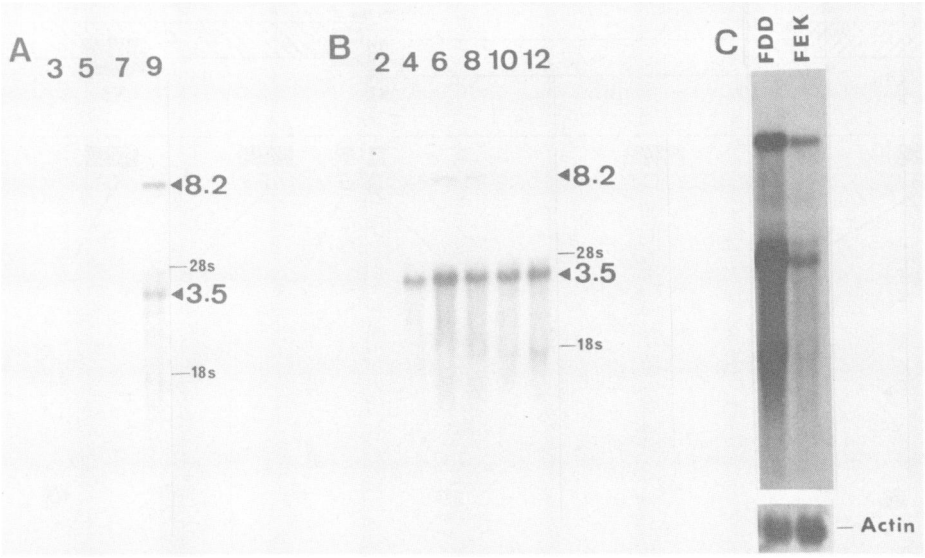

FIG. 5. Time course study on the synthesis of EIAV-specific transcripts. The numbers above each lane in panels A and B correspond to the times at which total RNA was isolated from infected cells (days postinfection). (A) Northern blot of total RNA isolated from FEK cells infected with prototype EIAV. (B) Northern blot of total RNA isolated from FDD cells infected with FDD-adapted EIAV. (C) Comparative Northern blot of total RNA from prototype EIAV-infected FEK or FDD-adapted EIAV-infected FDD cells. In panels A and B, 15.0 μg of total RNA, isolated at each time point, was loaded on the appropriate lane of the gel. The positions of the 8.2- and the 3.5-kb viral RNAs and of the 28S and 18S rRNAs are indicated. In panel C, 15.0 μg of total RNA, isolated from infected FEK cells at 14 days postinfection and from infected FDD cells at 12 days postinfection, was loaded on each appropriate lane. All three blots were hybridized to a mixture of ^{32}P-labeled probes A and G. The probes were then stripped from the blot shown in panel C, and the membrane was hybridized to a ^{32}P-labeled actin cDNA probe as an internal control for loading and transfer of the two RNA samples (lower insert).

abundance 1.5-kb RNA, detected at an even lower quantity in Northern blots of poly(A)$^+$ RNA isolated from infected FEK cells (data not shown), was not clearly observed in blots of total RNA from either infected cell line used in this time course analysis. This is probably due to the presence of large quantities of 18S rRNA in samples of total cellular RNA. However, it is evident that overproduction of the 3.5-kb spliced RNA occurs early in the cytopathic infection of FDD cells and does not appear to be temporally regulated. The relative quantities of viral RNAs in infected FEK and FDD cells were estimated from a comparative Northern blot (Fig. 5C). Densitometric analysis of this blot revealed that there was almost a 10-fold higher level of viral RNAs in infected FDD cells at the peak of the cytopathic effect relative to that in persistently infected FEK cells and that the 3.5-kb RNA constituted more than 75% of all viral RNA in infected FDD cells. Coupled with the asynchronous nature of viral infection in FDD cells (Table 1), we estimate the levels of EIAV-specific RNAs to be 30-fold higher during the cytopathic infection of FDD cells relative to the persistent infection of FEK cells. As an internal control for loading and transfer of equal quantities of the two RNA samples, the blot in Fig. 5C was stripped and rehybridized with an actin probe (Fig. 5C, lower panel).

***trans*-Activational regulation of the EIAV LTR in infected cells.** The association of multispliced, low-molecular-weight viral transcripts to *trans*-activational regulation of lentivirus gene expression (1, 2, 6, 21) and the low abundance of such RNAs in EIAV-infected cells raises questions as to whether viral *trans*-activating factor(s) are indeed expressed in these infected cell lines. *trans*-Activational regulation of EIAV gene expression has been previously reported to occur in Cf2Th and FEA cells persistently infected with EIAV (8, 9, 29). To ascertain whether the EIAV LTR is also activated in *trans* in the infected FEK and FDD cell lines used for the transcriptional studies presented so far, standard *trans*-activation assays utilizing the EIAV LTR-driven bacterial CAT gene were performed on these two fibroblastic cell lines of equine origin, using the infected Cf2Th and FEA cells as controls. As shown in Fig. 6, the levels of EIAV LTR-regulated CAT expression were significantly enhanced in all four cell lines infected with EIAV compared with those in uninfected cells, confirming that *trans* activation of viral gene expression also occurs in infected FEK and FDD cells. Thus, it appears that although EIAV gene expression is under *trans*-activational regulation, subgenomic multispliced small viral mRNAs in the size range of 1.2 to 2.0 kb are detected at low abundance in persistent or cytopathic EIAV infections, in contrast to other lentivirus infections in which such mRNAs are produced in concentrations equivalent to those of the full-length and single-spliced mRNA species (2, 7, 21, 26, 33).

DISCUSSION

The present study was conducted to analyze and compare EIAV DNA and RNA synthesis during persistent and cytopathic infections. We have observed that during the persistent infection of FEK cells, 70% of the total EIAV proviral DNA is in unintegrated forms that are equally divided between a linear and a circular species; the remaining 30% of viral DNA is present as randomly integrated provirus. The two major detectable species of viral RNA, an 8.2-kb full-length genomic and a 3.5-kb subgenomic RNA, are present in approximately equal quantities in these persistently infected cells. During the cytopathic infection of FDD cells, however, 65 to more than 90% of the provirus is integrated, depending on the virus strain employed, with the remaining proviral DNA divided equally between unintegrated linear and circular forms. In addition to the two major viral

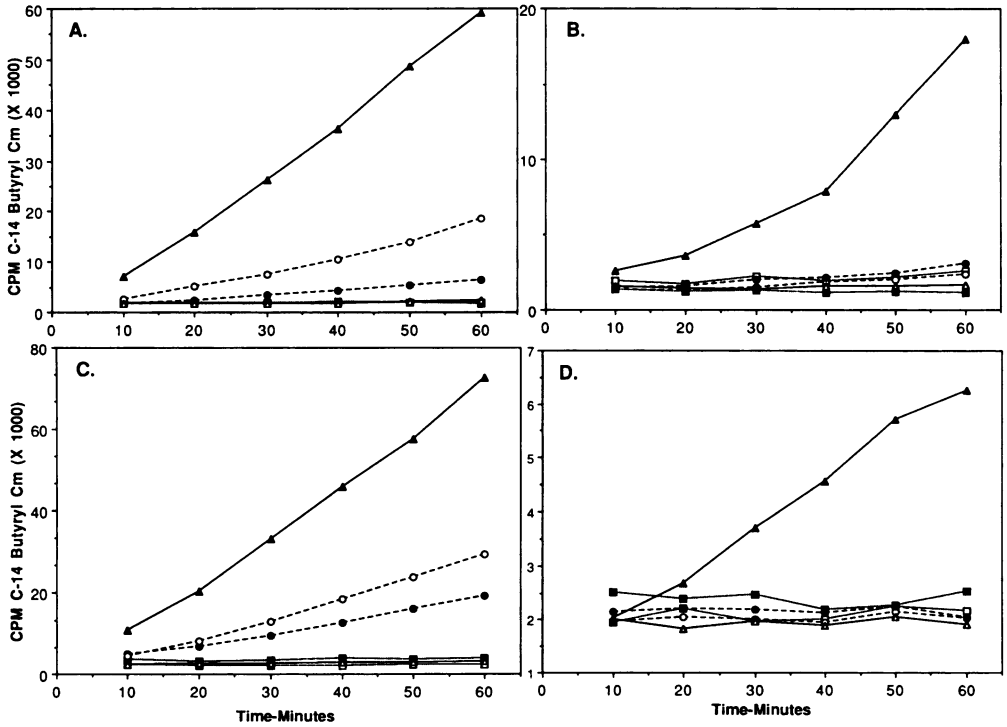

FIG. 6. Analysis of EIAV LTR-driven CAT activity in transfected FEA (A), Cf2Th (B), FDD (C), and FEK (D) cells. CAT assays were performed as described in Materials and Methods. Symbols: ■, pSV0CAT in EIAV-infected cells; □, pSV0CAT in uninfected cells; ●, pSV2CAT in EIAV-infected cells; ○, pSV2CAT in uninfected cells; ▲, pLTRCAT in EIAV-infected cells; △, pLTRCAT in uninfected cells.

transcripts observed in persistently infected FEK cells, a low-abundance 1.5-kb RNA is also detected in the cytopathic infection of FDD cells. Viral transcription appears to be much more efficient during the cytopathic infection, as the quantity of total viral RNA is nearly 30-fold higher than that detected in persistently infected cells. Moreover, during cytopathic infection, the spliced 3.5-kb RNA is the major viral transcript and constitutes over 75% of all viral RNA.

Several studies on the correlation of lentivirus DNA forms and pathogenesis have been described (3, 15, 22, 27). In general, these studies suggest that persistent, noncytopathic infections are associated with a predominance of integrated proviral DNA, while cytopathic infections display a predominance of unintegrated proviral DNA. For instance, previous studies have reported that the EIAV provirus is mainly integrated in cells isolated from infected horses and have proposed that the persistent, nonlytic infection of equine fibroblasts by EIAV could be due to this integration (3, 27). More recently, a similar mechanism has also been suggested for the chronic infection of the H9 human T-cell line by HIV-1 (22). Furthermore, it has been suggested that during the infection of sheep choroid plexus cells by visna virus, cell damage is due to an accumulation of unintegrated viral DNA (15), and during acute infection of human peripheral lymphocyte cultures by HIV-1, more than 400 copies per cell of linear unintegrated viral DNA have been reported to be present (22). The results obtained in the EIAV studies described here, however, appear to suggest that the ratio of integrated to unintegrated viral DNA increases when comparing the cytopathic infection of FDD cells with the persistent infection of FEK cells, and this ratio increases even further when the infectious agent is the FDD-adapted strain of EIAV which causes a more rapid cytopathic effect in infected FDD cells. These observations indicate that any generalized correlation of lentiviral DNA forms with replication and cytopathologic levels may not be justified at this time. Further studies of other lentiviruses, using various other cell lines, particularly those serving as target cells in vivo, are required to clarify this fundamental aspect of lentivirus molecular biology.

The splicing patterns of the lentivirus full-length RNA are generally believed to be more complex than those of other retroviruses, and studies on HIV-1 and visna virus point to the presence of a family of double-spliced viral mRNAs which, in general, encode a variety of *trans*-acting viral regulatory proteins (1, 2, 6, 7, 21, 22, 26, 33). The results of the studies on patterns of EIAV transcription presented here, however, appear to suggest a simpler transcriptional pattern which may correlate with the simpler genetic organization of EIAV relative to visna virus or HIV-1. The observed pattern of EIAV transcription points to an abundance of the 3.5-kb viral RNA and low levels of the presumably double-spliced 1.5-kb RNA during the cytopathic infection of FDD cells, along with equal ratios of the 8.2- and 3.5-kb RNAs and almost undetectable levels of the 1.5-kb RNA in persistently infected FEK cells. This differential transcriptional pattern of EIAV in the two cell lines examined suggests the involvement of a cell type-specific regulatory mechanism of viral transcription. It remains to be determined whether the more efficient splicing of the full-length EIAV genomic RNA to the 3.5-kb *env* transcript in infected FDD cells is a cell-specific phenomenon resulting from potential interactions between certain cellular factor(s) and viral regulatory protein(s). This in turn may affect the stability of the full-length viral RNA or its efficiency of transport from the nucleus to the cytoplasm relative to that of the 3.5-kb RNA. In the case of HIV-1, the *trans*-acting *rev* protein has already been proposed to have a role in trans-

porting the full-length and single-spliced viral RNAs to the cytoplasm and away from the splicing machinery in the nucleus (11, 14, 18). Furthermore, the enhanced levels of *env* mRNA in EIAV-infected FDD cells may result in higher levels of viral glycoprotein production in these cells, thus contributing to the cytopathic effects of the infection. In this regard, high-level expression of the HIV-1 envelope gene has been shown to have a direct role in syncytium formation and cytopathicity (30).

The functional role of the three short ORFs in the EIAV genome are not clearly understood at this time, although preliminary deletion studies have identified *S2* as an absolute requirement for *trans* activation of the EIAV LTR (9). Recent cDNA cloning and sequencing experiments from this laboratory have revealed the presence of a spliced viral mRNA in EIAV-infected FDD cells which is generated by splicing the first of three putative splice-donor sites located in the 5′ end of the EIAV *gag* gene to the putative splice acceptor site located upstream of the *env* gene, near the 5′ terminus of the *S1* reading frame (Fig. 4, genomic map; S. Rasty, unpublished data). The presence of AUG codons in both *S2* and *env* suggests that this mRNA could potentially code for *S2* in addition to allowing the translation of *env*, since the two genes are in different reading frames and their AUG codons are separated by 23 nucleotides. This mode of translation is in agreement with the translational model of Kozak (17) and could produce both the *S2* gene product and the viral glycoproteins from the same mRNA. We are currently testing this model by expression of this cDNA to identify its protein products and to ascertain any regulatory functions.

ACKNOWLEDGMENTS

This work was supported in part by funds from the Louisiana Agricultural Experiment Station, U.S. Department of Agriculture grant GM8502128, and Public Health Service grants CA38551 and AI25850 from the National Institutes of Health.

We thank Mark A. Miller for invaluable technical assistance.

LITERATURE CITED

1. **Arya, S. K., and R. C. Gallo.** 1986. Three novel genes of human T-lymphotropic virus type III: immune reactivity of their products with sera from acquired immune deficiency syndrome patients. Proc. Natl. Acad. Sci. USA **83**:2209–2213.
2. **Arya, S. K., C. Guo, S. F. Josephs, and F. Wong-Staal.** 1985. Transactivator gene of human T-lymphotropic virus type III (HTLV-III). Science **229**:60–73.
3. **Cheevers, W. P., S. G. Watson, and P. Klevjer-Anderson.** 1982. Persistent infection by equine infectious anemia virus: asymmetry of nucleotide sequence reiteration in the integrated provirus of persistently infected cells. Virology **118**:246–253.
4. **Chirgwin, J. M., A. E. Przybyl, R. J. MacDonald, and W. J. Rutter.** 1979. Isolation of biologically active ribonucleic acid from sources enriched in ribonuclease. Biochemistry **18**:5249–5299.
5. **Clements, J. E., O. Narayan, D. E. Griffin, and R. T. Johnson.** 1979. The synthesis and structure of visna virus DNA. Virology **93**:377–385.
6. **Davis, J. L., and J. E. Clements.** 1989. Characterization of a cDNA clone encoding the visna virus transactivating protein. Proc. Natl. Acad. Sci. USA **86**:414–418.
7. **Davis, J. L., S. Molineaux, and J. Clements.** 1987. Visna virus exhibits a complex transcriptional pattern: one aspect of gene expression shared with the acquired immunodeficiency syndrome retrovirus. J. Virol. **61**:1325–1331.
8. **Derse, D., P. L. Dorn, L. Levy, R. M. Stephens, N. R. Rice, and J. W. Casey.** 1987. Characterization of equine infectious anemia virus long terminal repeat. J. Virol. **61**:743–747.
9. **Dorn, P. L., and D. Derse.** 1988. *cis*- and *trans*-acting regulation of gene expression of equine infectious anemia virus. J. Virol. **62**:3522–3526.
10. **Feinberg, A. P., and B. Vogelstein.** 1983. A technique for radiolabeling DNA restriction endonuclease fragments to high specific activity. Anal. Biochem. **132**:6–13.
11. **Felber, B. K., M. Hadzopoulou-Cladras, C. Cladras, T. Copeland, and G. N. Pavlakis.** 1989. rev protein of human immunodeficiency virus type 1 affects the stability and transport of the viral mRNA. Proc. Natl. Acad. Sci. USA **86**:1495–1499.
12. **Fordis, C. M., and B. H. Howard.** 1987. Use of the CAT reporter gene for optimization of gene transfer into eukaryotic cells. Methods Enzymol. **151**:382–397.
13. **Gorman, C. M., L. F. Moffat, and B. H. Howard.** 1982. Recombinant genomes which express chloramphenicol acetyltransferase in mammalian cells. Mol. Cell. Biol. **2**:1044–1051.
14. **Hammarskjold, M.-L., J. Heimer, B. Hammarskjold, I. Sangwan, L. Albert, and D. Rekosh.** 1989. Regulation of human immunodeficiency virus *env* expression by the *rev* gene product. J. Virol. **63**:1959–1966.
15. **Harris, J. D., H. Blum, J. Scott, B. Traynor, P. Ventura, and A. Haase.** 1984. Slow virus visna: reproduction *in vitro* of virus from extrachromosomal DNA. Proc. Natl. Acad. Sci. USA **81**:7212–7215.
16. **Hirt, B.** 1967. Selective extraction of polyoma DNA from infected mouse cell cultures. J. Mol. Biol. **26**:365–369.
17. **Kozak, M.** 1986. Bifunctional messenger RNAs in eukaryotes. Cell **47**:481–483.
18. **Malim, M. H., J. Hauber, S.-Y. Lee, J. V. Maizel, and B. R. Cullen.** 1989. The HIV-1 *rev trans*-activator acts through a structured target sequence to activate nuclear export of unspliced viral mRNA. Nature (London) **338**:254–257.
19. **Malmquist, W. A., D. Barnett, and C. S. Becvar.** 1973. Production of equine infectious anemia antigen in a persistently infected cell line. Arch. Virol. **42**:361–370.
20. **Maniatis, T., E. F. Fritsch, and J. V. Sambrook.** 1982. Molecular cloning: a laboratory manual. Cold Spring Harbor Laboratory, Cold Spring Harbor, N.Y.
21. **Mazarin, V., I. Gourdou, G. Querat, N. Sauze, and R. Vigne.** 1988. Genetic structure and function of an early transcript of visna virus. J. Virol. **62**:4813–4818.
22. **Muesing, M. A., D. H. Smith, C. D. Cabradilla, C. V. Benton, L. A. Lasky, and D. J. Capon.** 1985. Nucleic acid structure and expression of the human AIDS/lymphadenopathy retrovirus. Nature (London) **313**:450–458.
23. **Neumann, J. R., C. A. Morency, and K. O. Russian.** 1987. A novel rapid assay for chloramphenicol acetyltransferase gene expression. BioTechniques **5**:444–447.
24. **Orrego, A., C. J. Issel, R. C. Montelaro, and W. V. Adams, Jr.** 1982. Virulance and in vitro growth of a cell-adapted strain of equine infectious anemia virus after serial passage in ponies. Am. J. Vet. Res. **43**:1556–1560.
25. **Payne, S. L., F.-D. Fang, C.-P. Liu, B. R. Dhruva, P. Rwambo, C. J. Issel, and R. C. Montelaro.** 1987. Antigenic variation and lentivirus persistence: variations in envelope gene sequences during EIAV infection resemble changes reported for sequential isolates of HIV. Virology **161**:321–331.
26. **Rabson, A. R., D. F. Daugherty, S. Venkatesan, K. E. Boulukos, S. I. Benn, T. M. Folks, P. Feorino, and M. A. Martin.** 1985. Transcription of novel open reading frames of AIDS retrovirus during infection of lymphocytes. Science **229**:1388–1390.
27. **Rice, N. R., S. Simek, O. A. Ryder, and L. Coggins.** 1978. Detection of proviral DNA in horse cells infected with equine infectious anemia virus. J. Virol. **26**:577–583.
28. **Rushlow, K., K. Olsen, G. Stiegler, S. L. Payne, R. C. Montelaro, and C. J. Issel.** 1986. Lentivirus genomic organization: the complete nucleotide sequence of the *env* gene region of equine infectious anemia virus. Virology **155**:309–321.
29. **Sherman, L., A. Gazit, A. Yaniv, T. Kawakami, J. E. Dahlberg, and S. R. Tronick.** 1988. Localization of sequences responsible for *trans*-activation of the equine infectious anemia virus long terminal repeat. J. Virol. **62**:120–126.
30. **Sodroski, J., W. C. Goh, C. Rosen, K. Campbell, and W. A.**

Haseltine. 1986. Role of the HTLV-III/LAV envelope in syncytium formation and cytopathicity. Nature (London) **322**:470–474.

31. **Stephens, R. M., J. W. Casey, and N. R. Rice.** 1986. Equine infectious anemia virus gag and pol genes: relatedness to visna and AIDS virus. Science **231**:589–594.
32. **Varmus, H. E.** 1982. Form and function of retroviral proviruses. Science **216**:812–820.
33. **Vigne, R., V. Barban, G. Querat, V. Mazarin, I. Gourdou, and N. Sauze.** 1987. Transcription of visna virus during its lytic cycle: evidence for a sequential early and late gene expression. Virology **161**:218–227.